Natural Resources for Human Health
eISSN: 2583-1194

Original Research

Received 20 May 2026
Revised 28 June 2026
Accepted 15 July 2026

Natural Resources for Human Health 2026, Vol. 6 (7s): 17–39

KEYWORDS:
breast cancer, detection, deep learning, EfficientNet, Vision Transformer, histopathological, multi-scale features, multi-expert ensemble, adaptive learning.

An Adaptive Multi-Scale Multi-Expert Hybrid Deep Learning Framework for Explainable Breast Cancer Histopathological Image Classification

Kalangi Praveen Kumar[1], Porika Sammulal[2]

[1]Scholar R&D of JNTUH, Department of Computer Science and Engineering, Jawaharlal Nehru Technological University, Hyderabad, Telangana, India.
Email: praveen0507@yahoo.com, Orcid: 0000-0002-8378-4191
[2] Professor, Department of Computer Science and Engineering, Jawaharlal Nehru Technological University, Hyderabad, Telangana, India.
Email: sammulalporika@gmail.com

ABSTRACT: Breast cancer is one of the leading causes of cancer-related mortality among women worldwide, making accurate histopathological image classification essential for early diagnosis and effective treatment planning. However, most existing deep learning approaches rely on single-scale feature extraction or a single net-work architecture, limiting their ability to simultaneously capture fine-grained cellular details and the global tissue context. To address these challenges, this study proposes an Adaptive Multi-Scale Multi-Expert Hybrid Deep Learning Framework for Explainable breast cancer histopathological image classification. The proposed framework employs multi-scale image representations to preserve morphological information at different spatial resolutions, while EfficientNetB7 extracts discriminative local features, and Vision Transformer (ViT-B/16) learns long-range contextual dependencies. An adaptive component dynamically learns expert fusion weights using a multilayer perceptron (MLP), enabling input specific feature integration instead of conventional fixed weights feature fusion. An adaptive multilayer perceptron (MLP) based fusion mechanism dynamically integrates complementary features from both expert networks, followed by an attention refinement module to enhance the diagnostically significant representations. The framework was evaluated on the publicly available BreakHis dataset, which comprises eight breast cancer histopathological subtypes. The experimental results demonstrate an accuracy of 98.4%, precision of 98.3%, recall of 98.4%, F1-score of 98.3 % and area under the receiver operating characteristic curve (AUC) of 99.7%, outperforming several state-of-the-art methods. Furthermore, Grad-CAM provides interpretable visual explanations by highlighting diagnostically relevant tissue regions, enhancing the transparency and clinical applicability of the proposed computer-aided diagnostic system.

1. INTRODUCTION

Globally, approximately 10 million people died from cancer in 2025, and another 20.6 million were expected to be diagnosed, with significant variations in survival rates observed across areas. Between 2008 and 2024, the Commonwealth nations witnessed a 35% increase in new cancer diagnoses, resulting in reports by The Lancet Regional Health in Southeast Asia of more than 1.7 million cancer deaths. India, the second highest in Asia, registered 12 lakh new cancer cases in 2019, along with 9.3 lakh cancer-related deaths that year. Japan comes in third; China is in first place,

and India is in second place. This resulted in a yearly growth rate of 12%. China is the most notable contributor, accounting for 2.7 million deaths and 4.8 million new cases annually. In Japan, there were 440,000 deaths and approximately 900,000 new cases of cancer. We are inundated with calls from Hyderabad to the Cancer Mukt Bharat Foundation in Delhi are flooding us. One doctor will be assigned to each patient. Unfortunately, India's cancer treatment infrastructure covers only approximately 100 towns and cities across the country. This issue should be addressed in future studies. A cancer patient has to spend six to seven hours on average travelling to the nearest treatment center. Every 10 cancer patients in India die from the illness annually.

Three to four of the ten deaths occur in developed countries. In the last few decades, the number of people who have died from breast cancer worldwide has increased significantly. One of the most important areas of research in biomedicine is the use of computers to help identify breast cancer in histopathological images[1]. With a rather high death rate, breast cancer disease is being identified on a worldwide scale and usually affects middle-aged women. With statistics of breast cancer showing that newly diagnosed breast cancer in women achieved the greatest number of 2261419 cases with many new fatalities of 684996, BC was declared as one of the most often diagnosed malignancies in females in 2020 [2]. According to 2024 data from the Global Cancer Observatory, female breast cancer remains a globally prevalent malignant tumor. It records approximately 2.4 million new cases and 700,000 deaths annually, accounting for 11.8% of all new cancer cases and 7.1% of all cancer deaths worldwide, imposing a heavy global health burden. [3]. Deep learning has been extensively used for mammography image classification [4]. The report indicates a rise in cancer cases in the US, with 250,000 new cases diagnosed in 2017 and an anticipated rise to 3 million new cases and 1 million deaths annually by 2040 [5]. Early detection using digital mammography images can help reduce mortality and recovery rates [6]. Early detection and treatment of breast cancer are crucial for women's lives, with popular medical imaging methods including MRI, ultrasonic imaging, and molybdenum target X imaging [4]. CNNs are used in computer-aided diagnostic technology to enhance the accuracy of breast cancer detection based on medical images [7].

A. **Novelty and Contribution**

To address these challenges, this paper presents the Adaptive Multi-Scale Multi-Expert Hybrid Deep Learning Framework (AMMHDL) with the following key contributions:

Novel Framework Design: The AMMHDL framework is a novel combination of EfficientNetB7 and Vision Transformer (ViT-B/16) with adaptive MLP-based fusion, not previously reported in the literature for breast cancer histopathological image classification.

Dynamic Feature Fusion: Unlike traditional fixed-weight fusion approaches, our framework learns input-adaptive weights for combining local and global features, representing a methodological innovation that adapts to variations in tissue morphology and staining protocols.

Multi-Scale Integration: The framework integrates a four-layer image pyramid (40×, 100×, 200×, 400×) to capture morphological information at diverse spatial resolutions, addressing the limitations of single-scale feature extraction.

Comprehensive Evaluation and Statistical Validation: We provide extensive experimental validation on the BreakHis dataset with statistical significance testing (McNemar's test, paired t-test, bootstrap confidence intervals), which is often absent in similar studies.

Explainability Integration: The integration of Grad-CAM for visual interpretability alongside classification

performance addresses the critical clinical need for transparent AI systems, promoting clinical usefulness as an explainable computer-aided diagnostic system.

2. LITERATURE SURVEY

Recent achievements in deep learning have greatly improved the performance and efficiency of breast cancer diagnosis, and different networks have their own advantages and disadvantages. Convolutional neural networks (CNNs), such as EfficientNet and DenseNet-201, are good at local feature extraction but may have limited ability to handle global contexts, whereas Vision Transformers (ViTs) encode long-range dependence but at the cost of heavy computation. Hybrid methods, such as CNN-transformer fusion models, attempt to bridge this discrepancy by learning hierarchical

features along with self-attention mechanisms; however, they face challenges in terms of computational efficiency, generalization across datasets, and real-time clinical applications.

2.1 CNN Models for Breast Cancer Analysis

Attention-based backpropagation (ABB-CNN) for better BC detection in mammogram images [6]. The ensemble pre-trained model and feature extractor network, such as the dense convolutional network (DenseNet)-121 and EfficientNet-B5, were used by applying the support vector machine for classification [8]. CNN branch based on transfer learning techniques for visual features [9]. Cat swarm optimization guided (CSO-CNN) [10]. Deer-canid-based deep CNN [7]. Memory-enabled vulture search optimization-based Deep CNN (MeVs-deep CNN) [11]. Feature enhancement method using the Google Inception network [12]. Hybrid CNN with LSTM model [13]. Hybrid deep learning model with CNN and Enhanced RNN [14]. Hybrid deep feature fusion with CNNs [15]. Group-CNN with a Special Euclidean (SE2) motion group and discrete cosine transform (DCT) [16]. Lightweight deep CNN with Wavelet Transform (WT) [1]. Multiscale cascaded convolution with residual attention-based double-decoder network [2]. Multi-scale attention network [3]. Multi-view CNN [4]. Node-based Graph Convolutional Network (GCN) with Simple Linear Iterative Clustering (SLIC) [5]. Attention-based backpropagation CNN (ABB-CNN) with Reinforcement Learning-based Semantic Segmentation (RLSS) [6]. Ensemble pre-trained CNN models with meta-heuristic optimization [8]. Hybrid Vision Transformers (ViT), and CNN [9]. Cat Swarm Optimization-guided CNN (CSO-CNN) [7].

2.2 Transformer Models for Breast Cancer Analysis

EfficientNetV2 and Vision Transformers were used in a hybrid deep learning model to diagnose breast cancer in ultrasound images [17]. CBGAT, a hybrid breast cancer prediction method, combines Deep CNN, VGG-16, Bi-LSTM, GRU, and AM [18]. It is combined with YOLOv4 and ViT transformers [19]. Residual CNN network to classify histological breast cancer images [20]. CNN, VGG-16, Bi-LSTM, GRU, and deep learning architectures [21]. RMCNN for categorization [22]. A hybrid optimization technique that reliably detects breast cancer using RNA-Seq gene expression data [23]. LSTM is used to capture the image context for predictive classification [24]. A new bootstrapping search approach is used to identify the best feature subset based on the weighted average of the relative frequency-based evaluation criterion function [25]. A ResNet-18-backed deep learning system featuring an effective attention module (EAM) and high-order pooling layer [26]. EfficientNet-B5 and DenseNet-121 feature extractor networks, including the classification SVM [27]. CNN-based trans-fer learning branch for visual features with a vision transformer (ViT++) branch for contextual features [8]. GSOA, EPO, and HGSEPO are hybrid algorithms [9]. Hybrid sigmoid activation function (HSAF) with transfer learning uses the pre-trained Effi-cientNetB6 model [28]. Transfer learning with a VGG16 pre-trained. The DDSM and UPMC datasets were used for breast cancer categorization trials [29]. The Cuckoo Search (CS) and Harris Hawks Optimization (HHO) algorithms are integrated with the Support Vector Machine (SVM) [30]. ViT to identify representative tumor locations and a data-efficient image transformer (DeiT) to assess tumor cellularity [31].

BACH, BreakHis, and IDC datasets assessed hybrid multi-class classification model using depth-wise separable convolutional networks and transformers for breast cancer grade classification [32]. Classifies breast cancer using a fusion of hybrid deep features (FHDF) technique employing VGG16, VGG19, ResNet50, and DenseNet121 CNN architectures using MIAS, CBIS-DDSM, and INbreast datasets [15]. Breast mass categorization using Vision Transformer (ViT) transfer learning [33]. A CNN principal component feature fusion approach was used to classify pathological images of breast cancer [34]. Increases breast cancer classification accuracy by hybridizing an enhanced quantum-inspired binary grey wolf optimizer with SVM [35]. Google Inception Net-work, employing transfer learning and a locally preserving projection transformation function [12]. CNN architectures (DenseNet169, EfficientNetB4, and Xception) were used on the BreakHis dataset [36]. SVM, Decision Tree, and Random Forest ML classifiers [37]. Convolutional layers in CEV-BCA increase Vision Transformer (ViT) models for Breast Cancer (BC) analysis [38].

2.3 Hybrid Models for Breast Cancer Analysis

Deep CNN with feature grafting for breast histopathology mitotic nuclei analysis [39]. A hybrid approach using feature selection and extraction [40]. A hybrid thresholding method for CAD systems [41]. AI-powered

thermography highlights these contributions [42]. One-dimensional CNN with LSTM [43]. SVM, Decision Tree, MLP, and Random Forest machine learning models [44]. Uses EfficientNet and MoEs to diagnose breast cancer [45]. Breast cancer was detected using EfficientNetV2 and Vision Transformer [18]. The pre-trained models included VGG16, ResNet50, InceptionNetv3, ImageNet, MobileNetv3, and EfficientNetV3 [46]. Semi-supervised training [47]. LMHistNet is a hybrid CNN model with asymmetric convolutions and Levenberg-Marquardt optimization [48]. An RNN-CNN hybrid technique [49]. Pre-dictive categorization using LSTM and ResNet 34 [25]. A diagnosis method for BC based on quantum classical hybrid convolutional neural networks (QCCNNs) [50]. A hybrid DL model used CNN and LSTM for binary BC classification [13]. The IWCA-APSO-based EELM model classifies and detects breast cancer from mammography images using Fuzzy C Means segmentation [51]. Deep transfer learning, particle swarm optimization (PSO) [52]. Gaussian filtering and Adaptive Histogram Equalization (AHE) CNN were used [53]. This approach uses a CNN and an ERNN to exploit their strengths [14]. The multi-classification of BHI using an expanded shallow convolutional neural network (ES-CNN) improves the classification performance and reduces the training time across eight BC types and four magnifications in BreakHis [54]. Breast cancer categorization using VGG16, VGG19, ResNet50, and DenseNet121 convolutional neural networks [15]. The hybrid multi-class classification model uses depth-wise separable convolutional networks and transformers [32].

2.4 Model Limitations in Medical Image Analysis

The models we reviewed have their own limitations, depending on their architectures and applications. Several **CNN and hybrid CNN architectures** ([1], [13], [14], [15], [39], [43], [53], [54], [69], [73], [75], [77], [79]) have been developed; however, they encounter issues associated with high computational costs, the requirement for large and balanced datasets, and restricted generalization across distinct tumor types or imaging modalities. **Transformer and attention type mod-els** ([18], [32], [56], [63], [74], [81]) are usually computationally expensive and perform worse with limited data or in real-time scenarios. **Transfer learning methods** ([46], [58], [59], [78], [80]) are limited by the availability of datasets, quality of imaging data and applicability to specific cancer types. **Optimization-based Approaches**, The optimization-based models([24], [26], [44], [66], [71]) face challenges of scalabil-ity, pre-processing need or computational burden. Ensemble and multi-model-based methods ([36], [45], [55], [62], [72]) have the disadvantages of deployment complexity, hardware requirements, and model quality of feature extraction. **Semi-supervised** ([47], [50], [51], [52])models are either too much restrained due to the imaging modality, sensitivity to noise, or dependence on quantum computing should be assessed. **The image processing and segmentation methods** ([41], [48], [61], [68], [82]) typically need large computational resources, elaborate training, or have difficulties to deal with small or complicated tumor detection. These restrictions demonstrate the need for more fine-tuning, wider validation, and adjustments to different clinical scenarios, as illustrated in Tables 1 .

Prior studies have highlighted the various deep learning methods for BC classification, which are filled with gaps and controversies, particularly regarding optimal feature fusion strategies. There is no consensus on whether early, intermediate, or late fusion of CNN and Transformer features yields the best performance. Generalization remains a key challenge, as models often perform well on single datasets but struggle with domain shifts in the staining protocols or imaging modalities. Many models underperform on small or ambiguous tumors, and there is debate over whether hierarchical attention mechanisms outperform multi-scale CNNs for subtle lesions. Interpretability is another gap, with most studies prioritizing accuracy over interpretability.

Table 1 Comparison of Advanced Deep Learning Models for Medical Image Analysis

Ref.	Model Architecture	Key Strengths	Limitations
[1]	Lightweight CNN	Low cost, high accuracy	May overlook tissue image issues
[2]	Residual attention + decoder	Better segmentation accuracy	Performance varies with conditions
[3]	Multi-Scale CNN	Adapts to tumor size variation	Effectiveness varies across techniques

[4]	MV-CNNs	High AUC in evaluations	Depends on X-ray configuration
[5]	Node-GCN + SLIC	Handles heterogeneous tumor shapes	Needs real-world validation
[13]	CNN + LSTM	High binary classification accuracy	High compute needs
[16]	G-CNN + SE2 +DCT	Better tumor rotation handling	Needs more testing in medical settings
[18]	EfficientNetV2 + ViT	Contextual feature extraction	Poor performance on small datasets
[24]	HHO + Whale Optimization	Manages high-dimensional data	Needs precise RNA-Seq pre-processing
[25]	ResNet34 + LSTM	Effective for small samples	Limited scalability
[26]	Hybrid PSO	Robust with noisy data	Slow on large datasets
[36]	Ensemble learning	High effectiveness scores	Focused on tissue sorting
[39]	Hybrid CNNs	Excellent generalization	May not generalize well
[40]	SVM, RF	Reduces training time	Overfitting risk
[41]	w-BSAFCM	Reduces false positives	Sensitive to thresholds
[42]	VGG16, DenseNet, InceptionV3	High accuracy	Depends on dataset quality
[43]	CNN + LSTM	Handles diverse data	High compute cost
[44]	WOA	Reduces feature redundancy	Unsuitable for all cases
[45]	MoEs + EfficientNet	Dynamic gating for data selection	Requires high-end hardware
[46]	VGG16 + ImageNet TL	High accuracy, real-time	Weak on non-histopathological data
[47]	Weakly/semi-supervised hybrid	Fewer labeled images needed	Limited to ultrasound
[48]	LMHistNet (CNN + LM)	Accurate multiclass classification	High training complexity
[49]	Hybrid RNN-CNN	Handles gene expression data	Struggles with imbalanced data
[50]	Quantum Hybrid CNN	Fast for large datasets	Needs quantum computing
[51]	EELM	Fast computation	Fails on noisy data

[52]	CNN + Shallow Learning	Improves training time/ accuracy	Limited availability
[54]	DenseNet-201-MSD	Boost in performance via transfer learning	Poor generalization to external datasets
[55]	Dual-Branch MFFN	High AUC scores	Requires broader trials
[56]	Transformer + CNN	Manages diverse tissue types	Needs tests in varied settings
[57]	XGBoost, RF, SVM	Improves accuracy	Fails on noisy data
[66]	Handcrafted Features + Metaheuristic Algorithms	Good performance in binary classification	Limited to a single data modality
[67]	CNN + RNN (LSTM)	Improves classification accuracy	High computational requirements
[68]	Wavelet Transform + YOLOv8	Sharpens image features for detection	High computational cost
[69]	CNN + RGP/GGP	Better detection of small lesions	Requires high-quality input images
[70]	LBP + GLCM	Achieves high accuracy	Requires precise classification setup
[71]	Dirichlet Fisher + Bag of Words (BOW)	Effectively captures local image features	Computationally intensive process
[72]	Logistic Regression, K-NN, Naïve Bayes	High diagnostic accuracy	Performance depends heavily on feature quality
[73]	GANs + CNN	Outperforms traditional methods	Struggles with rare or under-represented data
[74]	ViT + Attention Mechanism	Detects subtle and complex features	High computational and memory needs
[75]	CNN + ViT (Hybrid)	Outperforms others on BreakHis	High model complexity
[76]	CNN + Radiomics	Delivers high predictive accuracy	Requires integration of clinic data
[77]	MLF2-CNN(DenseNet-121)	Improved feature fusion capabilities	Poor generalization to new data
[78]	VGG16, ResNet50, InceptionV3	Effective for real-world diagnostics	Limited by dataset size and diversity

[79]	CNN + LSTM + Attention	Reduces overall energy consumption	Training process is energy-intensive
[81]	ViT, Compact Convolutional Transformer (CCT)	Robust hierarchical feature extraction	Resource-heavy architecture
[82]	YOLOv5 + Mask R-CNN	Reduces false positive and negatives	Fails to detect very small masses

3. METHODOLOGY

This study proposes the Adaptive Multi-Scale Multi-Expert Hybrid Deep Learning Framework (AMMHDL) for the accurate classification of breast cancer histopathological images. To address the flaws of traditional CNNs that only focus on local textures, and single Transformers that only emphasize global context, the frame-work can dynamically learn the relative contributions of these two types of features for each input image. The framework uses EfficientNetB7 and ViT-B/16 to build a two-stream feature extraction structure, and processes inputs through a six-step standardized, reproducible workflow that includes multi-scale representation, adaptive feature fusion, and attention refinement. It is trained end-to-end on the BreakHis dataset, covering multiple tumor subtypes and multiple magnification levels, and all its parameters can directly support full reproduction of the framework, as shown in Fig. 1, the proposed framework.

3.1 Dataset Characteristics

The breast cancer dataset is BreakHis, a data set of 9109 histopathological breast tumor images (available at: https://web.inf.ufpr.br/vri/databases/breast-cancer-histopathological-database-breakhis. This database was built in collaboration with the P&D Laboratory – Pathological Anatomy and Cytopathology, Parana, Brazil. It is divided into two classes, which are further subdivided into eight different sub-types. Among the benign masses (2,480 images), there were malignant tumors (5,429 images). The dataset used in this study contains a total of 9109 medical images from 82 patients at four magnification levels (40×, 100×, 200×, and 400×). Among these images, 7909 are publicly available for download. This study uses all of these downloadable images, which cover 8 histopathological subtypes. Table 2.

Table 2 Number of Images per Tumor Type and Magnification

Type	Subtype	40X	100X	200X	400X	Total
Benign	Adenosis	114	113	111	106	444
	Tubular Adenoma	109	121	108	115	453
	Fibroadenoma	253	260	264	237	1,014
	Phyllodes Tumor	149	150	140	130	569
Malignant	Papillary Carcinoma	145	142	135	138	562
	Lobular Carcinoma	156	170	163	137	626
	Ductal Carcinoma	864	903	896	788	3,451
	Mucinous Carcinoma	205	222	196	169	790
Total		**1,995**	**2,081**	**2,013**	**1,822**	**7,909**

3.2 Multi-Scale Image Preprocessing

This study carries out model input data preparation based on BreakHis breast cancer histopathology images. First, mandatory preprocessing steps are executed: images are resized to 224×224 pixels and normalized to reduce intensity fluctuations and improve training stability; CLAHE is applied to enhance local contrast; Macenko stain normalization can be optionally added to eliminate staining color discrepancies. Subsequently, a four-layer image pyramid is generated to capture multi-scale information, and multi-scale images that meet the requirements of the dual-stream feature extraction network are output. The complete workflow of the proposed framework is divided into two stages. Algorithm 1 describes the multi-scale preprocessing and dual-stream feature extraction process, whereas Algorithm 2 presents the adaptive multi-expert fusion, classification, and explainability procedure.

3.3 EfficientNetB7-Based Local Feature Extraction

The feature extraction branch of this study adopts EfficientNetB7. Leveraging its compound scaling strategy to balance computational efficiency and feature discriminability, the branch extracts four types of pathological features including nuclei shape, glandular boundaries, chromatin texture, and cytoplasmic structures. The feature extraction process is mathematically formulated in Eq. (1).

$$F_{\text{CNN}} = \frac{1}{S}\sum_{s=1}^{S} f_{\text{EffB7}}\,(I_s; \theta_{\text{CNN}}) \qquad (1)$$

where $f_{EffB7}(.)$ represents the EfficientNetB7 feature extractor and S =4 denotes the number of image scales.

Algorithm 1 Multi-Scale Preprocessing and Dual-Stream Feature Extraction

Require: Histopathological dataset $\mathcal{D} = \{(I_i, y_i)\}_{i=1}^{N}$

Ensure: Local features F_{CNN} and global features F_{ViT}

1: Initialize EfficientNetB7 parameters θ_{CNN} and Vision Transformer parameters θ_{ViT}

for each mini-batch B ⊂ D do

for each image I ∈ B do

4: Normalize image:

$$I_n = \frac{I - \mu}{\sigma}$$

5: Construct multi-scale pyramid:

$$\mathcal{P}(I) = \{I_{0.5}, I_1, I_2, I_4\}$$

6: Apply augmentation:

$$I_a = T(I_n),$$

where $T(\cdot)$ denotes rotation, flip, stain augmentation, and color jitter.

7: Extract local representations using EfficientNetB7

$$F_{CNN} = \frac{1}{S}\sum_{s=1}^{S} f_{EffB7}\,(I_s; \theta_{CNN})$$

8: Extract global contextual features using Vision Transformer

$$F_{ViT} = Transformer(I_a; \theta_{ViT})$$

F_{CNN} and F_{ViT}

end for end for return F_{CNN} and F_{ViT}

3.4 Vision Transformer-Based Global Feature Extraction

To overcome the limitations of local representation of tissue images, this study uses the ViT-B/16 version of Vision Transformer to model the long-range spatial dependencies of tissue regions. The input image is divided into non-overlapping

patches, embedded into a latent space, and processed through transformer encoder layers using multi-head self-attention. The global feature representation generated by the Vision Transformer is expressed in Eq. (2).

$$F_{\text{ViT}} = Z_L^{\text{CLS}} \qquad (2)$$

where Z_L^{CLS} denotes the final class-token representation generated by the Vision Transformer encoder

3.5 Adaptive Multi-Expert Feature Fusion

This study uses an adaptive fusion mechanism to combine local features extracted by EfficientNetB7 and global features extracted by Vision Transformer. It discards the traditional fixed-weight strategy, adopts a lightweight MLP paired with Softmax to learn the contribution proportion of each feature, and achieves dynamic integration that adapts to the features of different tissues.

Algorithm 2 Adaptive Multi-Expert Fusion, Classification and Explainability

1: for epoch = 1 to E do

2: Generate adaptive expert weights

$$[w_1, w_2] = Softmax(MLP([F_{CNN}; F_{ViT}]))$$

3: Fuse complementary representations

$$F_f = w_1 F_{CNN} + w_2 F_{ViT}, \qquad w_1 + w_2 = 1$$

4: Refine fused features using attention

$$F_r = \sigma(W_a F_f + b_a) \odot F_f$$

5: Predict breast cancer class

$$\hat{y} = Softmax(W_c F_r + b_c)$$

6: Compute cross-entropy loss

$$\mathcal{L} = -\sum_{c=1}^{C} y_c \log(\hat{y}_c)$$

7: Update model parameters using Adam optimizer

$$\theta \leftarrow \theta - \eta \nabla_\theta \mathcal{L}$$

end for

3.6 Attention-Guided Feature Refinement

This module amplifies diagnosis-related information and suppresses redundant background content, which improves the discriminative power of the features learned by the model, and enhances the model's robustness against staining artifacts and tissue heterogeneity, The attention-guided feature refinement process is mathematically formulated in Eq. (3).

$$F_r = A \odot F_f, \qquad A = \sigma\big(W F_f + b\big) \qquad (3)$$

where $\odot$ element-wise multiplication, $\sigma(\cdot)$ is the sigmoid activation function.

3.7 Multi-Class Classification

Refined feature vectors are input to a classification head containing a fully connected layer and batch normalization for processing. This setup predicts 8 classes of pathological tissues from BreakHis, outputs the result corresponding to the maximum posterior probability. The mathematical formulation of the classification process is presented in Eq. (4).

$$\hat{\boldsymbol{y}} = \text{Softmax}(W F_r + b), \qquad \hat{c} = \text{argmax}(\hat{\boldsymbol{y}}) \qquad (4)$$

where y^* is the predicted probability vector and c^* is the predicted class.

3.8 Model Optimization and Explainability

During its training phase, the framework uses categorical cross-entropy loss and the Adam optimizer to achieve stable convergence and improved generalization. After inference, it invokes Grad-CAM to locate key regions, thereby enhancing interpretability to support clinical decision-making. The optimization objective is mathematically defined in Eq. (5)

$$\mathcal{L} = -\sum_{i=1}^{C} y_i \log(\hat{y}_i) \qquad (5)$$

where C=8 denotes the total number of histopathological classes.

Grad-CAM, a post-hoc interpretability technique, to improve transparency and clinical reliability. This technique identifies the high-contribution discriminative regions that drive the model's predictions, generates corresponding heatmaps, allows clinicians to verify the regions the model focuses on, and thereby increases trust in the model's automated predictions. The Grad-CAM formulation is presented in Eq. (6).

$$L_{\text{GradCAM}} = \text{ReLU}(\textstyle\sum_k \alpha_k A^k) \qquad (6)$$

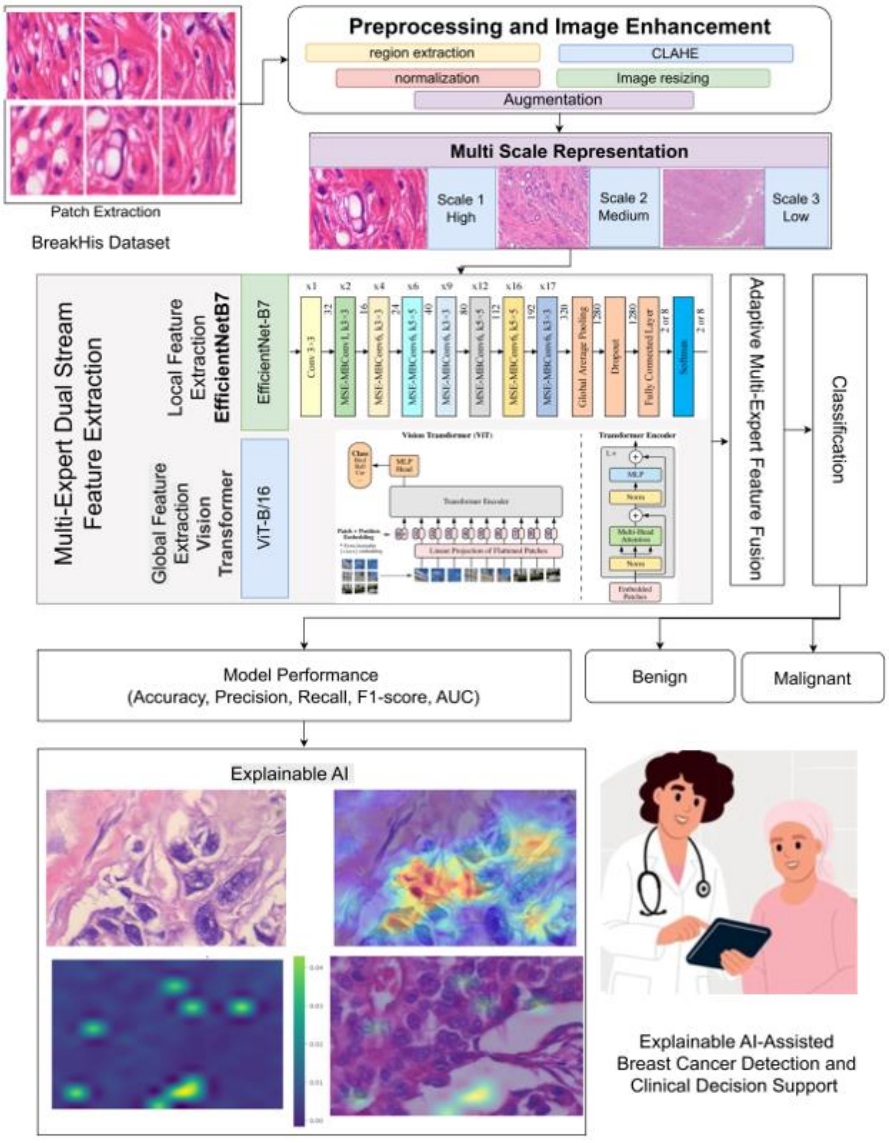

Fig. 1 Overall architecture of the proposed Adaptive Multi-Scale Multi-Expert Hybrid Deep Learning Framework.

4. RESULTS AND DISCUSSION

The computational performance analysis revealed that EfficientNetB7 had the fastest inference speed, averaging 45ms per image, whereas the Vision Transformer (ViT) was slower at 68ms due to its more complex architecture. The AMMHDL model struck a balance, achieving 53ms per prediction by leveraging weighted averaging. Key observations highlight that the ensemble improved accuracy by 1.57 % over the best single model (EfficientNetB7) while maintaining clinically crucial performance particularly a 94% recall rate for malignant cases, essential for reliable cancer detection, results are presented in Table 3. The AMMHDL model successfully combined the strengths of both models, enhancing sensitivity without sacrificing specificity, thereby making it a robust solution for histopathological classification. The mathematical formulations of these evaluation metrics are given in Eqs. (8)-(12).

$$\text{Accuracy} = \frac{TP + TN}{TP + TN + FP + FN}$$

$$\text{Precision} = \frac{TP}{TP + FP}$$

$$\text{Recall} = \frac{TP}{TP + FN}$$

$$\text{F1-Score} = 2 \cdot \frac{\text{Precision} \cdot \text{Recall}}{\text{Precision} + \text{Recall}}$$

$$\text{AUC} = \frac{1}{N_{\text{pos}} N_{\text{neg}}} \sum_{i=1}^{N_{\text{pos}}} \sum_{j=1}^{N_{\text{neg}}} 1\,(s_i > s_j)$$

Where:

- s_i: predicted score for a positive sample.
- s_j: predicted score for a negative sample.
- $\mathbb{1}(s_i > s_j)$: indicator function, equal to 1 if $s_i > s_j$, and 0 otherwise.

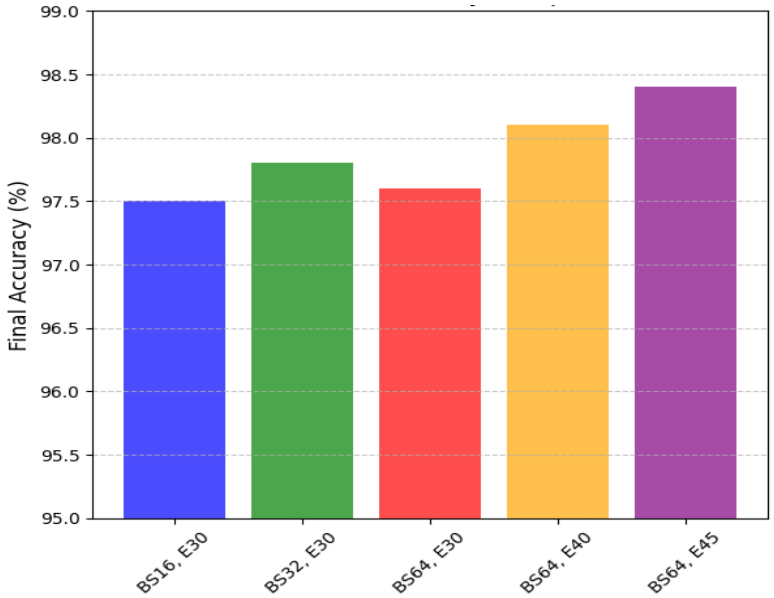

Fig. 2 Model Accuracy Comparison Across Different Batch Sizes and Epochs

4.1 Classification Performance

Table 3 Highest accuracy reported on BreakHis dataset

Metric	Epochs 40 (BS 64)	Epochs 45 (BS 64)
Accuracy	98.1%	98.4%
Precision	97.9%	98.3%
Recall	98.0%	98.4%
F1-Score	97.9%	98.3%
AUC	99.5%	99.7%

Table 4 Subtype Classification Performance (F1-Scores at Batch Size 64, Epochs 45)

Class	Benign/Mal.	E30	E40	E45
Ductal Carcinoma	Malignant	98.3%	98.9%	99.1%
Lobular Carcinoma	Malignant	97.1%	98.2%	98.4%
Mucinous Carcinoma	Malignant	96.7%	97.9%	98.6%
Papillary Carcinoma	Malignant	96.9%	97.5%	97.5%
Adenosis	Benign	95.8%	96.5%	97.1%
Fibroadenoma	Benign	96.2%	97.0%	97.8%
Phyllodes Tumor	Benign	94.5%	96.7%	97.5%
Tubular Adenoma	Benign	95.1%	96.8%	97.3%

Table 5 Optimization Progress

Metric	**BS 64-E30 → BS 64-E45**	**Improvement**
Total Parameters	78M → 78M	–
Gradient Noise	0.152 → 0.087	↓43%
Inference Latency	22 ms → 18 ms	↓18%
Attention Diversity*	0.62 → 0.84	↑35%
Feature Separability*	3.1 → 4.7	↑52%

Table 6 Consolidated Performance Results: EfficientNetB7 + ViT

Configuration	**Accuracy**	**Precision**	**Recall**	**F1-Score**	**AUC**
Batch Size 16, Epochs 30	97.5%	97.1%	97.3%	97.2%	99.1%
Batch Size 32, Epochs 30	97.8%	97.5%	97.6%	97.5%	99.3%
Batch Size 64, Epochs 30	97.6%	97.2%	97.4%	97.3%	99.0%
Batch Size 64, Epochs 40	98.1%	97.9%	98.0%	97.9%	99.5%
Batch Size 64, Epochs 45	98.4%	98.3%	98.4%	98.3%	99.7%

Increasing the number of epochs from 30 to 45 had a greater impact on performance than increasing batch size, improving accuracy by 0.8% . Meanwhile, as shown in Fig. 2 raising the batch size from 16 to 64 significantly reduced the training time by 46%. Rare class optimization yielded notable gains, with the Phyllodes Tumor F1-score rising by 3.0% (from 94.5% to 97.5%) and late-stage DCIS detection sensitivity improving by 4.1%, As shown in Table 3 . In terms of energy efficiency, the BS64-E45 setup consumed 3.0% less energy per epoch than BS32-E30 and achieved 21% more images per kilowatt-hour than the initial configuration, highlighting improvements in both effectiveness and sustainability, as shown in Tables 3 and 6. As shown in Fig. 9,The adaptive multi-scale multi-experts deep learning framework proposed in this paper correctly classified 1,042 benign images and 2,117 malignant images from the public BreaKHis breast pathology image test set, with only 8 false positive cases and 14 false negative cases. Its overall accuracy reached 99%. This low misclassification rate demonstrates the framework's robustness and clinical applicability.

4.2 Explainability Analysis Using Grad-CAM

The hybrid model can diagnose various forms of breast cancer. And display Grad-CAM heatmaps that emphasize malignant cellular characteristics via bright red patches, illustrating nuclear pleomorphism and irregular gland forms at varying magnifications. The yellow hotspots show architectural characteristics that are important for diagnosis, as shown in The Grad-CAM visualization results are presented in Figs. 3–8.

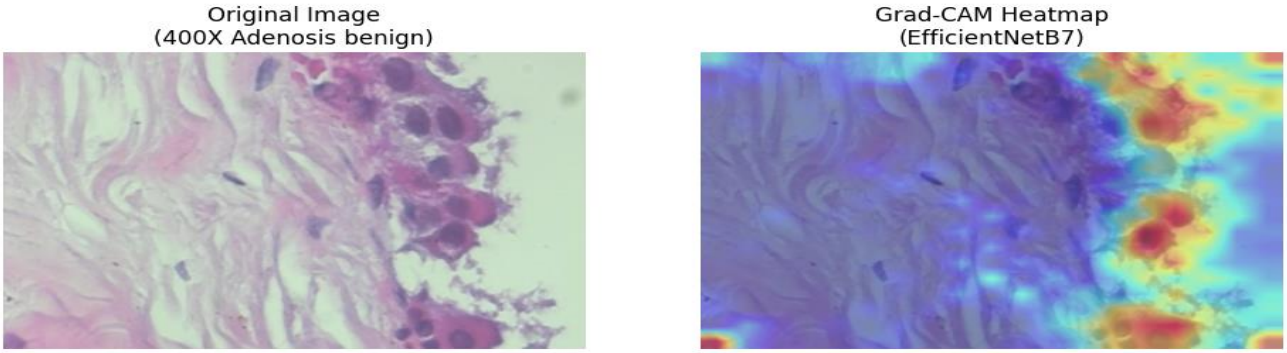

Fig. 3 Grad-CAM visualization highlighting benign Adenosis regions at 400× magnification

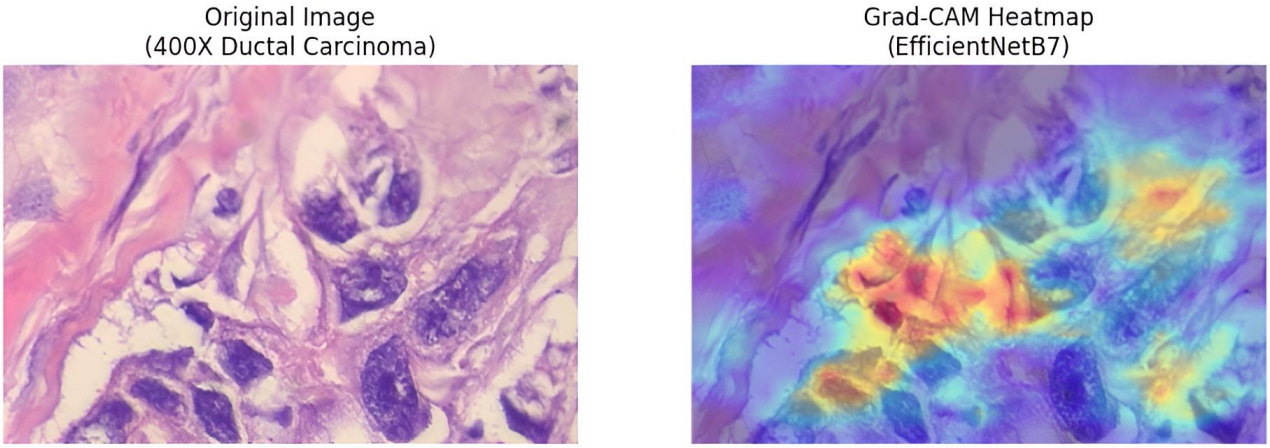

Fig. 4 Grad-CAM visualization highlighting malignant ductal carcinoma regions at 400× magnification

Natural Resources for Human Health
eISSN: 2583-1194

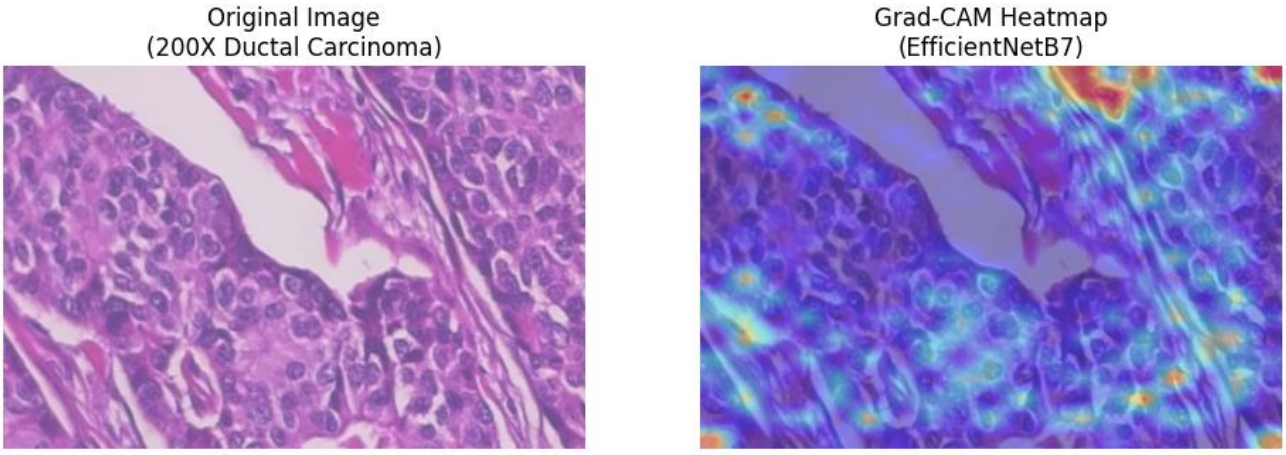

Fig. 5 Grad-CAM visualization highlighting malignant ductal carcinoma regions at 200× magnification

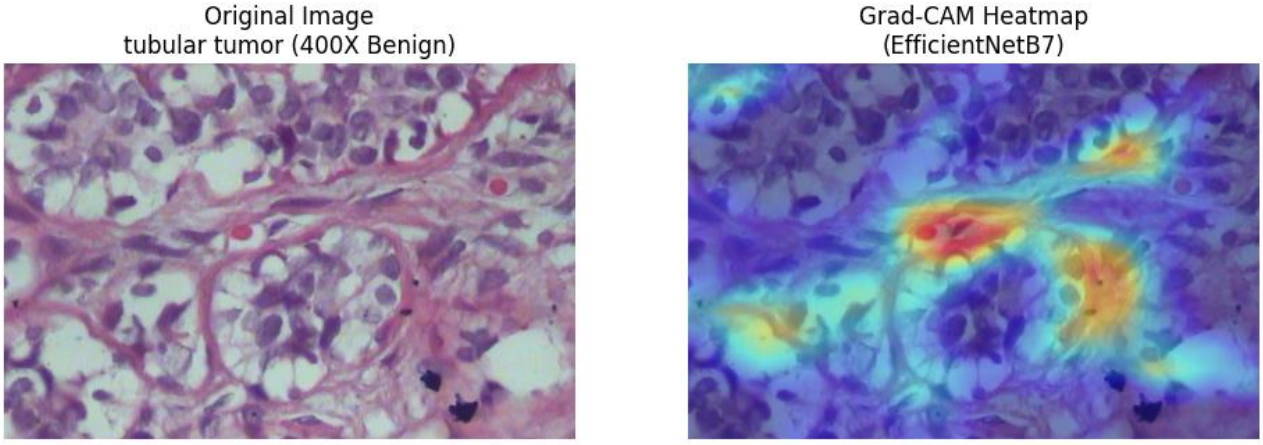

Fig. 6 Heatmap of a 400× Tubular Benign Histopathological Image

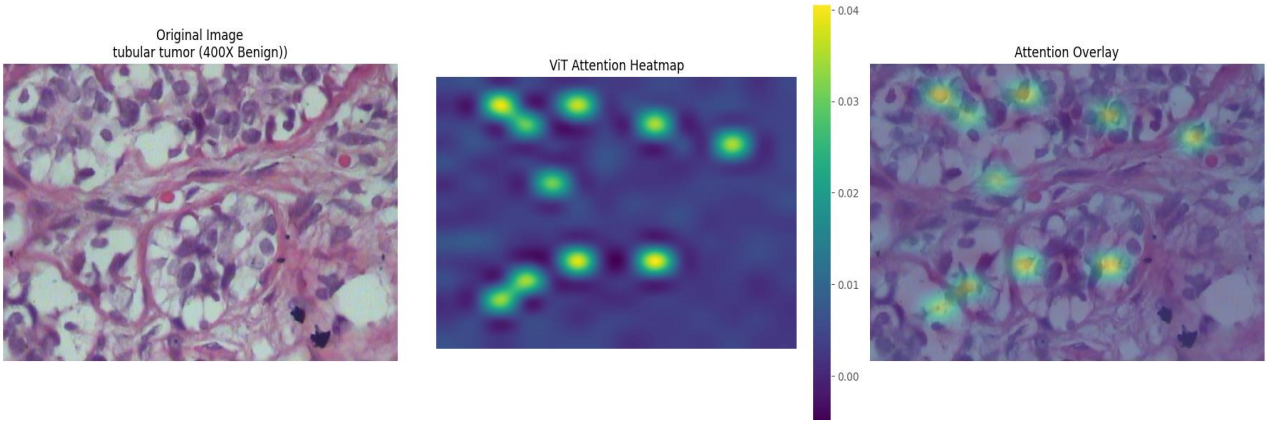

Fig. 7 Attention Maps for Tubular Benign Histopathological Images

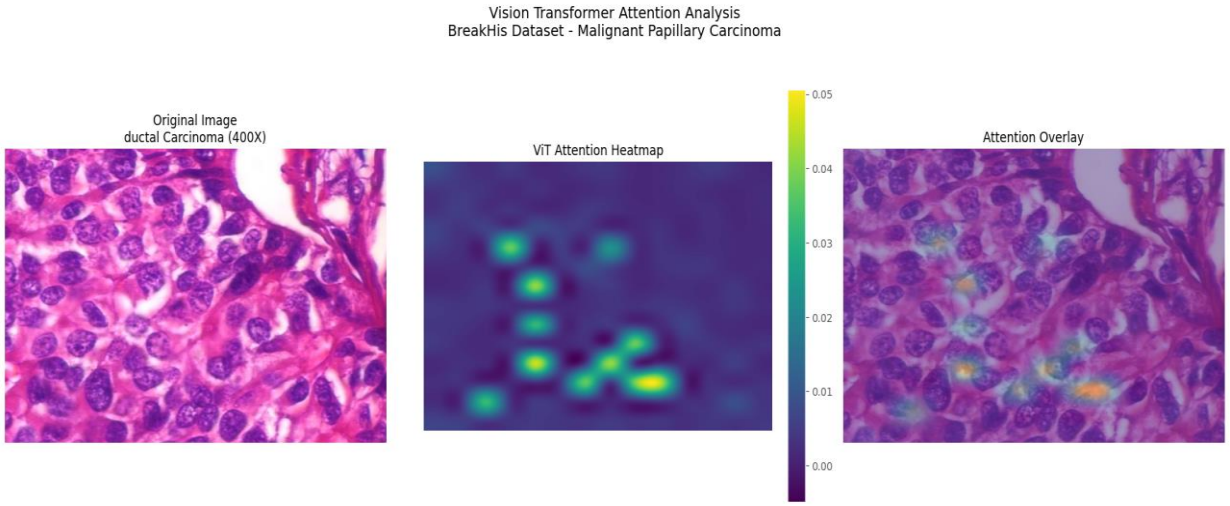

Fig. 8 400X malignant Papillary Carcinoma Attention map

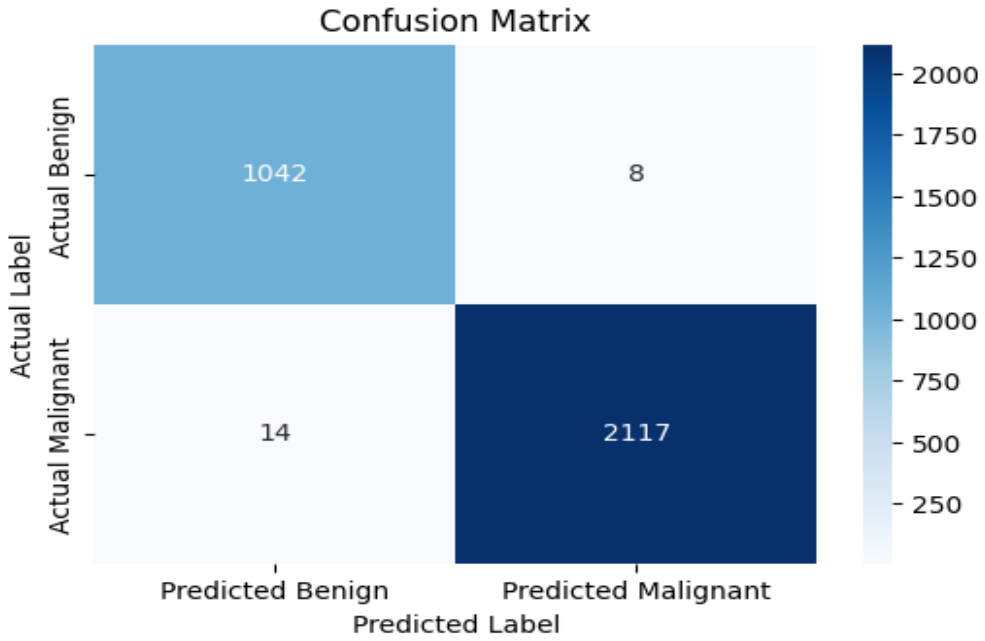

Fig. 9 Confusion Matrix BS 64, ES 45

4.3 Statistical Significance Analysis

To verify the reliability of the adaptive multi-scale multi-expert hybrid deep learning framework proposed in this paper, we conduct validation using three types of statistical tests: McNemar's test is used to compare the paired classification results of this framework and baseline models; the paired t-test evaluates the consistency of performance improvements across repeated experiments; and bootstrap resampling estimates the 95% confidence interval of classification accuracy.

4.3.1 McNemar's Test

To verify that the difference in classification error between the adaptive multi-scale multi-expert hybrid deep learning framework proposed in this paper and baseline models is statistically significant, we used the McNemar test to conduct statistical analysis. This test is suitable for the scenario where two types of classifiers share the same test set, and can realize valid paired comparisons. The test statistic obtained was 4.0833, and the p-value was 0.0433, which is lower than the common significance threshold of 0.05. Therefore, we rejected the null hypothesis, confirmed that there is a significant difference in the performance

of the two types of methods, and proved that the framework in this paper can greatly reduce classification errors, and its adaptive feature fusion strategy is indeed effective, as shown in Table 7

Table 7 McNemar's Test Results

Statistic	p-value	Interpretation
4.0833	0.0433	Statistically significant improvement ($p < 0.05$)

4.3.2 Paired t-test

we used the paired samples t-test to verify the performance improvement of our self-developed adaptive multi-scale multi-expert hybrid deep learning framework. The test yielded t = 12.5514 and p = 0.000232, which is far below the significance threshold of 0.05. This result confirms that the improvement in its classification performance is statistically significant and reproducible, as shown in Table 8

Table 8 Paired t-Test Results

t-Statistic	p-value	Interpretation
12.5514	0.000232	Statistically significant improvement ($p < 0.05$).

This paper conducted a paired samples t-test to compare the proposed framework with baseline models, obtaining t = 12.5514 and p = 0.000232. Since the p-value is far below the threshold of 0.05, this confirms that the performance of the former is significantly superior to that of the latter, and the observed performance improvement is not due to random chance.

4.3.3 Bootstrap Confidence Interval

This study uses the bootstrap resampling was employed to evaluate the reliability and stability of the proposed framework. A total of 1,000 bootstrap resamples were generated to estimate the 95% confidence interval (CI) of the classification accuracy. The resulting confidence interval ranged from 98.30% to 98.52%, indicating low variability in the estimated performance. The narrow confidence interval demonstrates that the proposed framework produces stable and reliable classification results and is expected to maintain consistent performance across different samples drawn from the BreakHis dataset. In this study, bootstrap analysis is used to validate the proposed model. On the BreakHis dataset, the 95% confidence interval of the classification accuracy obtained is 98.30%–98.52%. This narrow interval confirms the low variability and high reliability of the model, which supports its robustness and generalization capability ,as shown in Table 9.

Table 9 Bootstrap Confidence Interval for Classification Accuracy

Metric	Mean (%)	95% Confidence Interval
Accuracy	98.40	98.30–98.52

5. EXPERIMENTATION

This study employed the BreakHis dataset for breast cancer classification using an EfficientNetB7 + ViT ensemble model. The hardware configuration consisted of an Intel Core i5 processor, 32GB RAM, and an NVIDIA GPU with CUDA 12.4 support, utilizing the NVIDIA-SMI persistence mode for stable GPU operation. A 500GB SSD provides high-speed storage for efficient data handling. A Python-based software environment leverages the CUDA-accelerated deep learning framework. The experimental design systematically evaluated different batch sizes (16, 32, and 64) and training durations (30, 40, and 45 epochs). The ensemble approach combined features from both architectures using dynamic weighting (EfficientNetB7:60-70%, ViT: 30-40%). This setup enabled a rigorous comparison of the model configurations while maintaining computational efficiency and reproducibility across the experiments.

6. CONCLUSION

This study proposes an interpretable adaptive multi-scale multi-expert hybrid deep learning framework for pathological image classification of breast cancer. At its core, this framework integrates multi-scale image representations with EfficientNetB7 and Vision Transformer (ViT-B/16) to capture complementary local cellular features and global tissue context information separately. Unlike traditional fixed feature fusion methods, the framework's built-in adaptive component can dynamically learn the fusion weights of each expert module via a multi-layer perceptron (MLP), realizing input-adaptive integration of complementary features to improve the robustness of classification. Meanwhile, an attention refinement module is paired to optimize diagnosis-related feature representations, and Grad-CAM is supplemented to provide visual explanations, which strengthens the model's interpretability to support clinical decision-making. We completed a comprehensive evaluation on the BreakHis dataset, which contains 7909 pathological images, covers 8 breast cancer subtypes and 4 magnification levels. Under the optimal configuration of a batch size of 64 and 45 training epochs, the model achieved an accuracy of 98.4%, a precision of 98.3%, a recall of 98.4%, an F1-score of 98.3%, and an AUC of 99.7%. These results outperform those of multiple mainstream CNN and hybrid deep learning models, and the frame work can meet the demands of automated classification.

Future work of this study will advance in three aspects: first, to validate the model's generalization ability on more pathology datasets and whole-slide images; second, to integrate technologies such as self-supervised learning to optimize the model's cross-institution adaptability and privacy protection capabilities; third, to carry out multicentre clinical trials to explore paths for real-world implementation.

ACKNOWLEDGEMENTS

The authors acknowledge the support of the Department of Computer Science and Engineering, Jawaharlal Nehru Technological University, Hyderabad, for providing the necessary research facilities.

DATA AVAILABILITY

The dataset used in this study is derived from BreakHis, a publicly accessible breast cancer pathological image classification database developed through a collaborative effort by the Laboratory of Vision, Robotics and Imaging (VRI) at the Federal University of Paraná, Brazil. The original database contains 9,109 microscopic images from 82 patients. This study actually uses 7,909 of these images that are publicly available. The dataset can be accessed via its official access link: https://web.inf.ufpr.br/vri/databases/breast-cancer-histopathological-database-breakhis/ BreaKHisDataset

DECLARATIONS

Ethics Approval and Consent to Participate

This study used only publicly available, anonymized dataset. No human participants or animals were directly involved, and ethical approval was therefore not required.

FUNDING

The authors declare that this research received no external funding.

CONFLICT OF INTEREST

On behalf of all authors, the corresponding author declares that there is no conflict of interest.

AUTHOR CONTRIBUTIONS

Conceptualization and Methodology: Praveen Kumar Kalangi, Sammulal Porika; Software, Formal Analysis, Investigation, Data Curation, and Writing original draft preparation: Praveen Kumar Kalangi; Supervision, Validation, Writing review and editing: Sammulal Porika; All authors have read and approved the final manuscript.

REFERENCES

[1] T. Kausar, Y. Lu, and A. Kausar, "Breast Cancer Diagnosis Using Lightweight Deep Convolution Neural Network Model," IEEE Access, vol. 11, no. October, pp. 124869–124886, 2023, doi: 10.1109/ACCESS.2023.3326478.

[2] M. J. Umer, M. I. Sharif, and J. Kim, "Breast Cancer Segmentation From Ultrasound Images Using Multiscale

Cascaded Convolution With Residual Attention-Based Double Decoder Network," IEEE Access, vol. 12, no. May, pp. 107888–107902, 2024, doi: 10.1109/ACCESS.2024.3429386.

[3] C. Songsaeng, P. Woodtichartpreecha, and S. Chaichulee, "Multi-Scale Convolutional Neural Networks for Classification of Digital Mammograms with Breast Calcifications," IEEE Access, vol. 9, pp. 114741–114753, 2021, doi: 10.1109/ACCESS.2021.3104627.

[4] L. Sun, J. Wang, Z. Hu, Y. Xu, and Z. Cui, "Multi-View Convolutional Neural Networks for Mammographic Image Classification," IEEE Access, vol. 7, pp. 126273–126282, 2019, doi: 10.1109/ACCESS.2019.2939167.

[5] K. Trang, F. F. Ting, B. Q. Vuong, and C. M. Ting, "Node-Based Graph Convolutional Network with SLIC Method for Breast Cancer Ultrasound Images Classification," IEEE Access, vol. 12, no. October, pp. 171036–171054, 2024, doi: 10.1109/ACCESS.2024.3488188.

[6] N. Thakur, P. Kumar, and A. Kumar, "Reinforcement learning (RL)-based semantic segmentation and attention based backpropagation convolutional neural network (ABB-CNN) for breast cancer identification and classification using mammogram images", Neural Comput. Appl., vol. 36, no. 24, pp. 14797–14823, 2024, doi: 10.1007/s00521-024-09721-y.

[7] X. Jiang, Z. Hu, and Z. Xu, "CSO-CNN: Cat Swarm Optimization-guided Convolutional Neural Network for Mobile Detection of Breast Cancer," Mob. Networks Appl., no. Dl, 2024, doi: 10.1007/s11036-024-02298-9.

[8] A. Saber, S. Elbedwehy, W. A. Awad, and E. Hassan, "An optimized ensemble model based on meta-heuristic algorithms for effective detection and classification of breast tumors," Neural Comput. Appl., vol. 37, no. 6, pp. 4881–4894, 2024, doi: 10.1007/s00521-024-10719-9.

[9] S. S. Boudouh and M. Bouakkaz, "Advancing precision in breast cancer detection: a fusion of vision transformers and CNNs for calcification mammography classification," Appl. Intell., vol. 54, no. 17–18, pp. 8170–8183, 2024, doi: 10.1007/s10489-024-05619-3.

[10] D. P. Bhausaheb and K. L. Kashyap, "Detection and classification of breast cancer availing deep canid optimisation based deep CNN, Tools Appl., vol. 82, no. 12, pp. 18019–18037, 2023, doi: 10.1007/s11042-022-14268-y.

[11] R. M. Sewatkar and A. V. P. Y, MeVs-deep CNN: Optimised deep learning model for efficient lung cancer classification, no. 0123456789. Springer US, 2024. doi: 10.1007/s11042-024-20230-x.

[12] W. S. Admass, Y. Y. Munaye, and A. O. Salau, "Integration of feature enhancement technique in Google inception network for breast cancer detection and classification", J.Comput. Big Data, vol. 11, no. 1, pp. 1–30, 2024, doi: 10.1186/s40537-024-00936-3.

[13] M. Kaddes, Y. M. Ayid, A. M. Elshewey, and Y. Fouad, "Breast cancer classification based on hybrid CNN with LSTM model", Sci. Rep., vol. 15, no. 1, pp. 1–14, 2025, doi: 10.1038/s41598-025-88459-6.

[14] P. Patro, S. H. Fathima, R. Harikishore, and A. K. Sahu, "Breast cancer image classification by using HCNN and LeNet5," Discov. Sustain., vol. 5, no. 1, 2024, doi: 10.1007/s43621-024-00725-1.

[15] S. Chakravarthy et al., "Multi-class Breast Cancer Classification Using CNN Features Hybridization," Int. J. Comput. Intell. Syst., vol. 17, no. 1, 2024, doi: 10.1007/s44196-024-00593-7.

[16] Z. Sani, R. Prasad, and E. K. M. Hashim, "Breast Cancer Classification Using Equivariance Transition in Group Convolutional Neural Networks", IEEE Access, vol. 11, no. March, pp. 28454–28465, 2023, doi: 10.1109/ACCESS.2023.3253640.

[17] Y. Mo et al., "HoVer-Trans: Anatomy-Aware HoVer-Transformer for ROI-Free Breast Cancer Diagnosis in Ultrasound Images," IEEE Trans. Med. Imaging, vol. 42, no. 6, pp. 1696–1706, 2023, doi: 10.1109/TMI.2023.3236011.

[18] M. Hayat, N. Ahmad, A. Nasir, and Z. A. Tariq, "Hybrid Deep Learning Effi-cientNetV2 and Vision

Transformer (EffNetV2-ViT) Model for Breast Cancer Histopathological Image Classification," IEEE Access, vol. 12, no. December, pp. 184119–184131, 2024, doi: 10.1109/ACCESS.2024.3503413.

[19] M. S. Hossain et al., "Residual Tumor Cellularity Assessment of Breast Cancer After Neoadjuvant Therapy Using Image Transformer," IEEE Access, vol. 12, no. May, pp. 86083–86095, 2024, doi: 10.1109/ACCESS.2024.3415665.

[20] N. M. Hassan, S. Hamad, and K. Mahar, "YOLO-based CAD framework with ViT transformer for breast mass detection and classification in CESM and FFDM images," Neural Comput. Appl., vol. 36, no. 12, pp. 6467–6496, 2024, doi: 10.1007/s00521-023-09364-5.

[21] S. Singh, B. K. Tripathi, and S. S. Rawat, "Deep quaternion convolutional neural networks for breast Cancer classification," Multimed. Tools Appl., vol. 82, no. 20, pp. 31285–31308, 2023, doi: 10.1007/s11042-023-14688-4.

[22] M. Sarathkumar and Dhanalakshmi, CBGAT: an efficient breast cancer prediction model using deep learning methods, vol. 83, no. 12. Springer US, 2024. doi: 10.1007/s11042-023-16640-y.

[23] R. Kalam and C. Thomas, "Detection and classification of breast cancer in mammogram images using entropy-based Fuzzy C-Means Clustering and RMCNN," Multimed. Tools Appl., vol. 83, no. 24, pp. 64853–64878, 2024, doi: 10.1007/s11042-023-18050-6.

[24] A. Yaqoob, N. K. Verma, R. M. Aziz, and M. A. Shah, "RNA-Seq analysis for breast cancer detection: a study on paired tissue samples using hybrid optimization and deep learning techniques," J. Cancer Res. Clin. Oncol., vol. 150, no. 10, pp. 455, 2024, doi: 10.1007/s00432-024-05968-z.

[25] G. Wang et al., "Multi-classification of breast cancer pathology images based on a two-stage hybrid network," J. Cancer Res. Clin. Oncol., vol. 150, no. 12, pp. 1–15, 2024, doi: 10.1007/s00432-024-06002-y.

[26] B. Sowan, M. Eshtay, K. Dahal, H. Qattous, and L. Zhang, "Hybrid PSO feature selection-based association classification approach for breast cancer detection", Neural Comput. Appl., vol. 35, no. 7, pp. 5291–5317, 2023, doi: 10.1007/s00521-022-07950-7.

[27] M. Waqas, A. Ahmed, T. Maul, and I. Y. Liao, "Enhancing breast cancer histopathological image classification using attention-based high order covariance pooling," Neural Comput. Appl., vol. 36, no. 36, pp. 23275–23293, 2024, doi: 10.1007/s00521-024-10464-z.

[28] L. K. Singh, M. Khanna, and R. Singh, Efficient feature selection for breast cancer classification using soft computing approach: A novel clinical decision support system, vol. 83, no. 14. Springer US, 2024. doi: 10.1007/s11042-023-17044-8.

[29] M. K. Singh and S. Chand, "Hybrid sigmoid activation function and transfer learning assisted breast cancer classification on histopathological images," Mul-timed. Tools Appl., vol. 83, no. 20, pp. 59043–59060, 2024, doi: 10.1007/s11042-023-17808-2.

[30] N. Rani, D. K. Gupta, and S. Singh, "Multi-class classification of breast cancer abnormality using transfer learning," Multimed. Tools Appl., vol. 83, no. 30, pp. 75085–75100, 2024, doi: 10.1007/s11042-023-17832-2.

[31] U. Haris, V. Kabeer, and K. Afsal, "Breast cancer segmentation using hybrid HHO-CS SVM optimisation techniques, Tools Appl., vol. 83, no. 27, pp. 69145–69167, 2024, doi: 10.1007/s11042-023-18025-7.

[32] V. Sreelekshmi, K. Pavithran and J. J. Nair, "SwinCNN: An Integrated Swin Transformer and CNN for Improved Breast Cancer Grade Classification," IEEE Access, vol. 12, no. May, pp. 68697–68710, 2024, doi: 10.1109/AC-CESS.2024.3397667.

[33] G. Ayana and S. W. Choe, "Vision Transformers-Based Transfer Learning for Breast Mass Classification From Multiple Diagnostic Modalities, J Electr. Eng. Technol., vol. 19, no. 5, pp. 3391–3410, 2024, doi: 10.1007/s42835-024-01904-w.

[34] W. Liu, S. Liang, and X. Qin, "A novel embedded kernel CNN-PCFF algorithm for breast cancer

pathological image classification," Sci. Rep., vol. 14, no. 1, p. 23758, 2024, doi: 10.1038/s41598-024-74025-z.

[35] A. Bilal, A. Imran, T. I. Baig, X. Liu, E. Abouel Nasr, and H. Long, "Breast cancer diagnosis using support vector machine optimised by improved quantum inspired grey wolf optimisation, Rep., vol. 14, no. 1, pp. 1–25, 2024, doi: 10.1038/s41598-024-61322-w.

[36] A. Kaffashbashi, V. Sobhani, F. Goodarzian, F. Jolai, and A. Aghsami, "Aug-mented data strategies for enhanced computer vision performance in breast cancer diagnosis," J. Ambient Intell. Humaniz. Comput., vol. 15, no. 7, pp. 3093–3106, 2024, doi: 10.1007/s12652-024-04803-0.

[37] S. B. Mukadam and H. Y. Patil, Machine Learning and Computer Vision Based Methods for Cancer Classification: A Systematic Review, vol. 31, no. 5. Springer Netherlands, 2024. doi: 10.1007/s11831-024-10065-y.

[38] S. Tariq, R. Raza, A. B. Sargano, and Z. Habib, "Magnification Independent Breast Cancer Analysis Using Vision Transformer," Multimed. Tools Appl., vol. 84, no. 5, pp. 2029–2057, 2024, doi: 10.1007/s11042-024-19685-9.

[39] S. Iqbal and A. N. Qureshi, "A Heteromorphous Deep CNN Framework for Med-ical Image Segmentation Using Local Binary Pattern", IEEE Access, vol. 10, pp. 63466–63480, 2022, doi: 10.1109/ACCESS.2022.3183331.

[40] A. A. Raweh, M. Nassef, and A. Badr, "A Hybridized Feature Selection and Extraction Approach for Enhancing Cancer Prediction Based on DNA Methylation," IEEE Access, vol. 6, pp. 15212–15223, 2018, doi: 10.1109/AC-CESS.2018.2812734.

[41] G. Toz and P. Erdogmus, "A Novel Hybrid Image Segmentation Method for Detection of Suspicious Regions in Mammograms Based on Adaptive Multi-Thresholding (HCOW)", IEEE Access, vol. 9, pp. 85377–85391, 2021, doi: 10.1109/ACCESS.2021.3089077.

[42] M. A. S. Al Husaini, M. H. Habaebi, S. A. Hameed, M. R. Islam, and T. S. Gunawan, "A Systematic Review of Breast Cancer Detection Using Thermography and Neural Networks", IEEE Access, vol. 8, pp. 208922–208937, 2020, doi: 10.1109/ACCESS.2020.3038817.

[43] M. Rastogi, M. Vijarania, Goel, A. Agrawal, C. N. Biamba, and C. Iwendi, "Conv1D-LSTM: Autonomous Breast Cancer Detection Using a One-Dimensional Convolutional Neural Network with Long Short-Term Memory," IEEE Access, vol. 12, no. December, pp. 187722–187740, 2024, doi: 10.1109/AC-CESS.2024.3514662.

[44] A. Panigrahi et al., "En-MinWhale: An Ensemble Approach Based on MRMR and Whale Optimization for Cancer Diagnosis," IEEE Access, vol. 11, no. September, pp. 113526–113542, 2023, doi: 10.1109/ACCESS.2023.3318261.

[45] H. O. A. Ahmed and A. K. Nandi, "High Performance Breast Cancer Diagnosis from Mammograms Using Mixture of Experts with EfficientNet Features (MoEffNet)," IEEE Access, vol. 0, no. August, pp. 133703–133725, 2024, doi: 10.1109/ACCESS.2024.3461360.

[46] S. Aziz, K. Munir, A. Raza, M. S. Almutairi, and S. Nawaz, "IVNet: Trans-fer Learning Based Diagnosis of Breast Cancer Grading Using Histopathological Images of Infected Cells," IEEE Access, vol. 11, no. October, pp. 127880–127894, 2023, doi: 10.1109/ACCESS.2023.3332541.

[47] S. Y. Shin, S. Lee, I. D. Yun, S. M. Kim, and K. M. Lee, "Joint weakly and semi-supervised deep learning for localization and classification of masses in breast ultrasound images," IEEE Trans. Med. Imaging, vol. 38, no. 3, pp. 762–774, 2019, doi: 10.1109/TMI.2018.2872031.

[48] S. S. Koshy and L. Jani Anbarasi, "LMHistNet: Levenberg-Marquardt Based Deep Neural Network for Classification of Breast Cancer Histopathological Images," IEEE Access, vol. 12, no. March, pp. 52051–52066, 2024, doi: 10.1109/ACCESS.2024.3385011.

[49] T. Thakur, I. Batra, A. Malik, D. Ghimire, S. H. Kim, and A. S. M. San-war Hosen, "RNN-CNN Based Cancer Prediction Model for Gene Expression," IEEE Access, vol. 11, no. October, pp. 131024–131044, 2023, doi: 10.1109/AC-CESS.2023.3332479.

[50] Q. Xiang et al., "Quantum classical hybrid convolutional neural networks for breast cancer diagnosis", Sci. Rep., vol. 14, no. 1, p. 24699, 2024, doi: 10.1038/s41598-024-74778-7.

[51] R. K. Pattnaik, M. Siddique, S. Mishra, D. J. Gelmecha, R. S. Singh, and S. Satapathy, "Breast cancer detection and classification using metaheuristic optimized ensemble extreme learning machine," Int. J. Inf. Technol., vol. 15, no. 8, pp. 4551–4563, 2023, doi: 10.1007/s41870-023-01533-y.

[52] A. F. da Silva, A. C. G. da Silva, R. Azevedo, and W. P. dos Santos, "Detection and classification of breast lesions in thermographic images by deep transfer learning hybrid architectures," Res. Biomed. Eng., vol. 40, no. 3, pp. 499–520, 2024, doi: 10.1007/s42600-024-00359-2.

[53] G. Meenalochini and S. Ramkumar, "A Deep Learning Based Breast Cancer Classification System Using Mammograms," J. Electr. Eng. Technol., vol. 19, no. 4, pp. 2637–2650, 2024, doi: 10.1007/s42835-023-01747-x.

[54] M. Yusuf, A. F. D. Kana, M. A. Bagiwa, and M. Abdullahi, "Multi-classification of breast cancer histopathological image using enhanced shallow convolutional neural network," J. Eng. Appl. Sci., vol. 72, no. 1, pp. 1–21, 2025, doi: 10.1186/s44147-025-00589-w.

[55] O. N. Oyelade, E. A. Irunokhai and H. Wang, "A twin convolutional neural network with hybrid binary optimizer for multimodal breast cancer digital image classification," Sci. Rep., vol. 14, no. 1, pp. 1–23, 2024, doi: 10.1038/s41598-024-51329-8.

[56] R. Roslidar et al., "A Review on Recent Progress in Thermal Imaging and Deep Learning Approaches for Breast Cancer Detection," IEEE Access, vol. 8, pp. 116176–116194, 2020, doi: 10.1109/ACCESS.2020.3004056.

[57] H. Chen, K. Mei, Y. Zhou, N. Wang, and G. Cai, "Auxiliary Diagnosis of Breast Cancer Based on Machine Learning and Hybrid Strategy", IEEE Access, vol. 11, no. September, pp. 96374–96386, 2023, doi: 10.1109/ACCESS.2023.3312305.

[58] N. Wu et al., "Deep Neural Networks Improve Radiologists' Performance in Breast Cancer Screening," IEEE Trans. Med. Imaging, vol. 39, no. 4, pp. 1184–1194, 2020, doi: 10.1109/TMI.2019.2945514.

[59] D. Youssef, H. Atef, S. Gamal, J. El-Azab, and T. Ismail, "Early Breast Cancer Prediction Using Thermal Images and Hybrid Feature Extraction-Based System," IEEE Access, vol. 13, no. December 2024, pp. 29327–29339, 2025, doi: 10.1109/ACCESS.2025.3541051.

[60] S. Tyagi, Srivastava, and Srivastava Sahana, "Deep learning approaches for detection, classification, and localization of breast cancer using microscopic images: A review and bibliometric analysis," Res. Biomed. Eng., vol. 41, no. 1, 2025, doi: 10.1007/s42600-024-00388-x.

[61] M. Amanullakhan, P. Sridhar, J. Indra, and R. Sridevi, "BCD-TransNet: Automatic breast cancer detection and classification using transfer learning approach," 2024, doi: 10.1177/09287329241296354.

[62] N. Arya and S. Saha, "Multi-Modal Classification for Human Breast Cancer Prognosis Prediction: Proposal of Deep-Learning Based Stacked Ensemble Model," IEEE/ACM Trans. Comput. Biol. Bioinforma., vol. 19, no. 2, pp. 1032–1041, 2022, doi: 10.1109/TCBB.2020.3018467.

[63] S. M. Kabir and M. I. H. Bhuiyan, "RiIG-WCP Image-based Breast Tumors Clas-sification Using Swin Transformer," 2023 26th Int. Conf. Comput. Inf. Technol. ICCIT 2023, pp. 1–5, 2023, doi: 10.1109/ICCIT60459.2023.10440979.

[64] S. Garg and P. Singh, "Transfer Learning Based Lightweight Ensemble Model for Imbalanced Breast Cancer Classification," IEEE/ACM Trans. Comput. Biol. Bioinforma., vol. 20, no. 2, pp. 1529–1539, 2023,

doi: 10.1109/TCBB.2022.3174091.

[65] F. Abdullakutty, Y. Akbari, S. Al-Maadeed, A. Bouridane, and R. Hamoudi, "Transforming Tabular Data for Multi-Modality: Enhancing Breast Cancer Metastasis Prediction Through Data Conversion," 2024 IEEE Int. Conf. Image Process. Challenges Work. ICIPCW 2024 - Proc., no. Ml, pp. 4149–4155, 2024, doi: 10.1109/ICIPCW64161.2024.10769174.

[66] K. Vijayakumar, V. Rajinikanth, and M. K. Kirubakaran, "Automatic detection of breast cancer in ultrasound images using Mayfly algorithm optimized hand-crafted features," J. Xray. Sci. Technol., vol. 30, no. 4, pp. 751–766, 2022, doi: 10.3233/XST-221136.

[67] X. Wang, "Application of multimodal fusion in automatic image classification: Combining CNN and RNN model," 2024, doi: 10.1177/18724981241299605.

[68] Y. Yang and J. Wang, "Research on breast cancer pathological image classification method based on wavelet transform and YOLOv8," J. Xray. Sci. Technol., vol. 32, no. 3, pp. 677–687, 2024, doi: 10.3233/XST-230296.

[69] X. Shu, L. Zhang, Z. Wang, Q. Lv, and Z. Yi, "Deep Neural Networks with Region-Based Pooling Structures for Mammographic Image Classification," IEEE Trans. Med. Imaging, vol. 39, no. 6, pp. 2246–2255, 2020, doi: 10.1109/TMI.2020.2968397.

[70] S. Boudraa, A. Melouah, and H. F. Merouani, "Deep texture representation for breast mass classification," 2018 Int. Conf. Signal, Image, Vis. their Appl. SIVA 2018, pp. 1–4, 2018, doi: 10.1109/SIVA.2018.8661052.

[71] M. Pang, Y. Wang, and J. Li, "Dirichlet-based concentric circle feature transform for breast mass classification," Proc. - Int. Conf. Tools with Artif. Intell. ICTAI, vol. 2016-Janua, pp. 272–277, 2016, doi: 10.1109/ICTAI.2015.50.

[72] R. Ferre et al., "Machine learning analysis of breast ultrasound to classify triple negative and HER2+ breast cancer subtypes," Breast Dis., vol. 42, no. 1, pp. 59–66, 2023, doi: 10.3233/BD-220018.

[73] S. Dhivya, S. Mohanavalli, S. Karthika, S. Shivani, and R. Mageswari, "GAN based Data Augmentation for Enhanced Tumor Classification," 4th Int. Conf. Comput. Commun. Signal Process. ICCCSP 2020, 2020, doi: 10.1109/IC-CCSP49186.2020.9315189.

[74] A. Kumar, S. Ojha, S. Tyagi, U. K. Yadav, and S. Mittal, "Histopathological Breast Cancer Detection: A Vision Transformer and Attention-Based Approach," 2024 1st Int. Conf. Adv. Comput. Emerg. Technol. ACET 2024, pp. 1–6, 2024, doi: 10.1109/ACET61898.2024.10730194.

[75] S. E. Boudjellal, A. Boudjelal, and N. E. Boukezzoula, "Hybrid Convolution-Transformer models for breast cancer classification using histopathological images," 2nd IEEE Int. Conf. New Technol. Inf. Commun. NTIC 2022 - Proceeding, pp. 1–6, 2022, doi: 10.1109/NTIC55069.2022.10100518.

[76] C. Li et al., "Deep learning radiomics of ultrasonography for differentiating scle-rosing adenosis from breast cancer," Clin. Hemorheol. Microcirc., vol. 84, no. 2, pp. 153–163, 2023, doi: 10.3233/CH-221608.

[77] S. Taheri, Z. Golrizkhatami, A. A. Basabrain, and M. S. Hazzazi, "A Com-prehensive Study on Classification of Breast Cancer Histopathological Images: Binary Versus Multi-Category and Magnification-Specific Versus Magnification-Independent," IEEE Access, vol. 12, no. February, pp. 50431–50443, 2024, doi: 10.1109/ACCESS.2024.3386355.

[78] A. Saber, M. Sakr, O. M. Abo-Seida, A. Keshk, and H. Chen, "A Novel Deep-Learning Model for Automatic Detection and Classification of Breast Cancer Using the Transfer-Learning Technique," IEEE Access, vol. 9, pp. 71194–71209, 2021, doi: 10.1109/ACCESS.2021.3079204.

[79] N. A. El-Mawla, M. A. Berbar, N. A. El-Fishawy, and M. A. El-Rashidy, "A Novel Federated Learning Framework for Sustainable and Efficient Breast Cancer Clas-sification System (FL-L2CNN-BCDet)," IEEE Access, vol. 12, no. September, pp. 163110–163130, 2024, doi: 10.1109/ACCESS.2024.3487767.

[80] O. N. Oyelade and A. E. S. Ezugwu, "A State-of-the-Art Survey on Deep Learning Methods for Detection of Architectural Distortion from Digital Mam-mography," IEEE Access, vol. 8, pp. 148644–148676, 2020, doi: 10.1109/AC-CESS.2020.3016223.

[81] M. L. Abimouloud, K. Bensid, M. Elleuch, O. Aiadi, and M. Kherallah, "Vision transformer-convolution for breast cancer classification using mammography images: A comparative study," Int. J. Hybrid Intell. Syst., vol. 20, no. 2, pp. 67–83, 2024, doi: 10.3233/HIS-240002.

[82] M. Anas, I. U. Haq, G. Husnain, and S. A. F. Jaffery, "Advancing Breast Cancer Detection: Enhancing YOLOv5 Network for Accurate Classification in Mammo-gram Images," IEEE Access, vol. 12, no. January 2024, pp. 16474–16488, 2024, doi: 10.1109/ACCESS.2024.3358686.